



# Multichannel SQUID Magnetoneurograph System for Functional Imaging of Spinal Cords and Peripheral Nerves

Yoshiaki Adachi (足立 善昭) , *Member, IEEE*, Shigenori Kawabata (川端 茂), Jun Hashimoto (橋本 淳), Yoshinori Okada (岡田 吉智), Yoshihisa Naijo (内城 禎久), Taishi Watanabe (渡部 泰士), Yuki Miyano (宮野 由貴), and Gen Uehara (上原 弦) , *Member, IEEE*

**Abstract**—We developed a superconducting quantum interference device (SQUID)-based biomagnetometer system for magnetoneurograms. The system was improved from a previously reported prototype magnetospinograph (MSG)/neurograph (MNG) system to satisfy the additional requirements that arose when we investigated practical clinical applications of the MSG/MNG in a hospital. The dimensions of the vector-type SQUID flux sensor array were increased to 150 mm × 188 mm, and the shape of the cryostat was modified so that the peripheral nerves at different body parts of a subject who assumed various postures, including positions provoking neurological symptoms, could be examined. In this paper, the improved MNG system is described in detail. Functional imaging of the brachial plexuses of subjects whose arms were in the abduction and external rotation position, which is one of the typical symptom-provocative positions for the shoulder, was achieved using the improved MNG system.

**Index Terms**—SQUIDS, biomedical imaging, biomedicine, magnetospinograph (MSG), magnetoneurograph (MNG).

## I. INTRODUCTION

**B** IOMAGNETIC measurement is a promising tool for non-invasively investigating the electrical activity in a living body. Weak magnetic fields accompanied by the activities of muscles or nerves penetrate the living organs because their permeability is almost constant and equivalent to that of a vacuum and are detected by multiple highly sensitive magnetic flux sensors arranged on the body surface. After the biomagnetic field

distribution is captured, a magnetic source analysis is performed to obtain the reconstructed current distribution, which reflects the functions of muscles and nerves. Magnetoencephalograms (MEGs) and magnetocardiograms (MCGs) are the established applications of the biomagnetic measurement. They have been utilized for functional imaging of the brain and heart, respectively. The intensity of the magnetic fields observed on the body surface is only a few pT. Therefore, superconducting quantum interference device (SQUID)-based flux sensors are used for detecting them in many practical applications [1], although “room-temperature” magnetic flux sensors have begun to be used for biomagnetic measurements [2]–[4].

We have been developing a SQUID biomagnetic measurement system for functional imaging of spinal cords, which came to be called the magnetospinograph (MSG). In 2007, we introduced the prototype of the MSG system for supine subjects [5]. The system was characterized by a uniquely shaped cryostat composed of a cylindrical main body to reserve liquid helium (LHe) and horizontal protrusion from its side surface. The SQUID sensor array was oriented vertically and arranged along the upper inner wall of the protrusion. This structure allowed the detection of magnetic field signals accompanied by spinal cord activity from the dorsal surface of a subject lying on a bed in a supine position.

The prototype of the MSG system has been operated at Tokyo Medical and Dental University Hospital for years and was demonstrated to be effective for the diagnosis of spinal cord diseases [6]. The shape of the sensor array and the protrusion of the cryostat were improved several times to capture the magnetic field distribution over a broader area. This is one of the requirements for the MSG at lumbar [7].

Recently, the application range of the MSG system was extended to functional imaging of peripheral nerves not only spinal cords. Therefore, the system came to be called a magnetoneurograph (MNG) system. Many pioneering studies on magnetoneurograms were performed in the early days of biomagnetic research [1], [8]–[11]. However, the clinical applications of the magnetoneurograms have not been developed to the extent of those of MEGs and MCGs. Owing to the unique structure of the sensor array and cryostat of our MSG system, the magnetoneurogram can be readily obtained by medical personnel, because any part of the body can be examined only if it can be placed on the

Manuscript received November 24, 2020; revised January 10, 2021; accepted January 29, 2021. Date of publication February 2, 2021; date of current version March 5, 2021. This work was supported in part by RICOH Company. (Corresponding author: Yoshiaki Adachi.)

Yoshiaki Adachi and Gen Uehara are with the Applied Electronics Laboratory, Kanazawa Institute of Technology, Kanazawa 920-1331, Japan (e-mail: adachi.y+iee@gmail.com).

Shigenori Kawabata is with the Department of Advanced Technology in Medicine, Graduate School of Tokyo Medical and Dental University, Bunkyo-ku 113-8510, Japan, and also with the Department of Orthopaedic Surgery of Tokyo Medical and Dental University, Bunkyo-ku 113-8510, Japan.

Jun Hashimoto is with the Department of Orthopaedic Surgery of Tokyo Medical and Dental University, Bunkyo-ku 113-8510, Japan.

Yoshinori Okada, Yoshihisa Naijo, Taishi Watanabe, and Yuki Miyano are with the Healthcare Business Group, RICOH Company, Chiyoda-ku 101-0062, Japan.

Color versions of one or more figures in this article are available at <https://doi.org/10.1109/TASC.2021.3056492>.

Digital Object Identifier 10.1109/TASC.2021.3056492

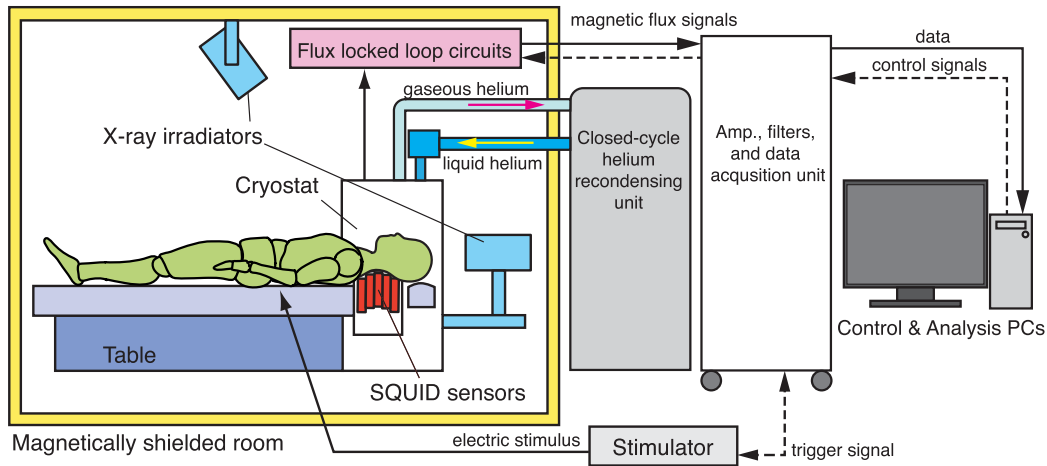


Fig. 1. Configuration of the SQUID MNG system.

sensor array. The software package to apply the artifact removal methods via signal processing [11], [12] and the current source estimation algorithm [13], which was originally developed for the MSG, was also effective for peripheral nerve measurements. Clinically valuable magnetoneurographic results, for example, visualization of the electrophysiological activity of the carpal tunnel area or brachial plexus, were obtained using our system [14], [15]. However, the imaging was performed only with neutral positioning. Although examinations with the positioning provoking symptoms are significantly more clinically important for peripheral nerves, they are often difficult because of the short distance between the sensor area and the cylindrical main body of the cryostat.

For the new multichannel SQUID system for functional imaging of spinal cords and peripheral nerves, the sensor array was expanded, and the shape of the cryostat was modified to satisfy the additional requirements that arose while the system was being operated for various clinical applications at the hospital. Using the new SQUID system, the magnetoneurographic measurement for brachial plexuses with symptom-provoking positioning, which is one of the largest requirements for clinical applications, was demonstrated.

## II. INSTRUMENTATION

### A. SQUID Sensor Array

Figure 1 shows the configuration of the developed MNG system. The basic structure of the system is similar to that of a previously reported system [16]. We focus on the sensor array and cryostat because they were improved from the previously-reported prototype. The sensor array was composed of 44 low-temperature SQUID flux sensors arranged in an area of  $150 \text{ mm} \times 188 \text{ mm}$  along a cylindrical surface with a radius of  $200 \text{ mm}$ , as shown in Fig. 2(a). The sensor area was expanded by  $>20\%$  even though the number of sensors was identical to that of the previous system. Each sensor module was equipped with three gradiometric pick-up coils made of niobium wire individually coupled with three LTS-SQUIDs. Therefore, the system was equipped with a 132-ch SQUID output. One of

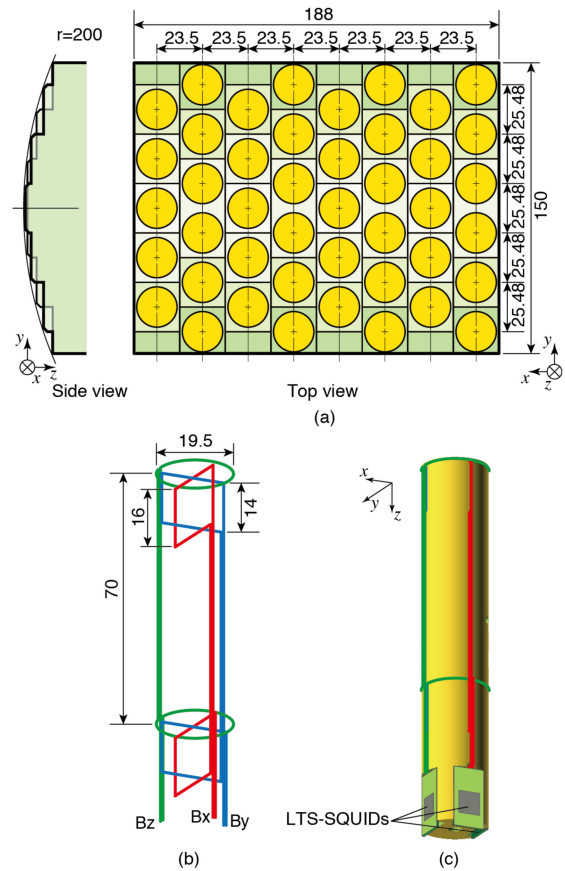


Fig. 2. (a) Dimensions of the sensor array. (b) Configuration and dimensions of gradiometric pick-up coils of a vector-type SQUID flux sensor. (c) Schematic of a vector-type SQUID flux sensor. All units are in mm.

the pick-up coils was an axial-type gradiometric coil and was used for detecting the component radial to the body surface. The other two pick-up coils were planar-type gradiometric coils to be used for detecting the tangential components. The dimensions of each pick-up coil were enlarged to improve the magnetic flux resolution relative to the previous prototype, as shown in Fig. 2(b). The coils were wound around a single bobbin and

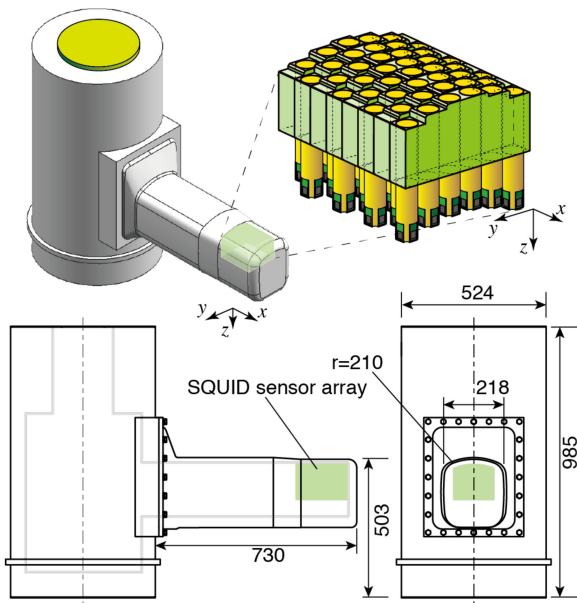


Fig. 3. Dimensions and appearance of the cryostat. All units are in mm.

oriented perpendicular to each other, as shown in Fig. 2(c). Each SQUID was driven by a triple-feedback flux-locked loop circuit to linearize the output and improve the dynamic range [16]. The typical noise level and frequency band were  $<2$  fT/Hz<sup>1/2</sup> in the white region and  $>2$  kHz, respectively.

### B. Cryostat

The design of the cryostat is similar to the conventional prototype of the MSG system for supine subjects [17], as shown in Fig. 3. However, the protrusion was extended to 730 mm because of two requirements that arose while the system was operated for various clinical applications in the hospital. The first requirement is to conduct measurements on large subjects such as football players. It was difficult for the conventional MSG system to examine a large person, because of the insufficient distance between the observation area and the surface of the cylindrical body. The second requirement is particularly significant for peripheral nerve measurements. Some patients complain of symptoms of pain or paralysis only when they assume certain positions, although the symptoms do not appear in neutral positioning. Therefore, it is important to allow measurements of different body parts of a subject who assumes various postures. The protrusion was extended along with the sensor array so that it would be easy to collect the signals from the brachial plexus of subjects whose arms were in the abduction and external rotation position, which is a typical symptom provocative position of the shoulder.

The sensor array oriented in a vertically upward direction was installed at the end of the protrusion along its upper inner surface, as well as the conventional prototypes. The cool-to-warm separation in the sensor array area was 12–14 mm. The capacity of the LHe was 92 L. The consumption rate of the LHe was approximately 9 L/d. Owing to the thermal uniformity in



Fig. 4. MNG measurement of the (a) right brachial plexus and (b) left brachial plexus. The white rectangles indicate the position of sensor area.

the cryostat, the SQUIDs could be operated although the LHe level was reduced below the level of the sensors.

### C. Peripherals

The new MNG system was equipped with the following peripherals as well as the previous prototypes for the MSG.

The anatomical information of the subjects is significant for magnetic source analysis and further clinical investigation. Two X-ray irradiators were set on the side of the cryostat and hung from the ceiling of the magnetically shielded room to obtain both lateral and coronal radiographic anatomical images, respectively, while the subject was placed on the sensor array. Marker coils were used for co-registration between the SQUID flux sensor array and the targeted body parts of the subjects projected onto the X-ray image, as well as co-registration between the conventional MEG and the magnetic resonance image [18]. The magnetically shielded room had a radiation shield layer made of a barium compound, in addition to the magnetic field and radiofrequency shield layers.

The cryostat was connected to the closed-cycle helium recondensing unit driven by a single pulse tube cryocooler, as well as the previous prototype [19]. The gaseous helium evaporating from the cryostat was recondensed to LHe and then returned to the cryostat. The maximum recondensing capacity was estimated as 14.4 L/d for an electrical power consumption of 8 kW. The noise from the cryocooler did not affect the MNG measurement even though it was adjacent to the magnetically shielded room. Because the signal frequency band of the MNG was  $>100$  Hz and did not overlap with the noise from the cryocooler, it could be readily removed by high-pass filters. Owing to the closed-cycle helium recondensing unit, almost 100% of the LHe was recycled.

## III. MNG MEASUREMENT

To verify of the system performance, a preliminary MNG recording of the brachial plexus was conducted. All the procedures in this study were approved by the Ethics Committee of Tokyo Medical and Dental University. The subjects were two males aged around 50 with no neurological symptoms. The subject laid on a bed in the abdominal position, with the right and left arms placed in an abduction and external rotation position one after another, as shown in Fig. 4. The subjects were able to readily assume this position owing to the improved cryostat. On-site X-ray images of the subjects' clavicle area were acquired



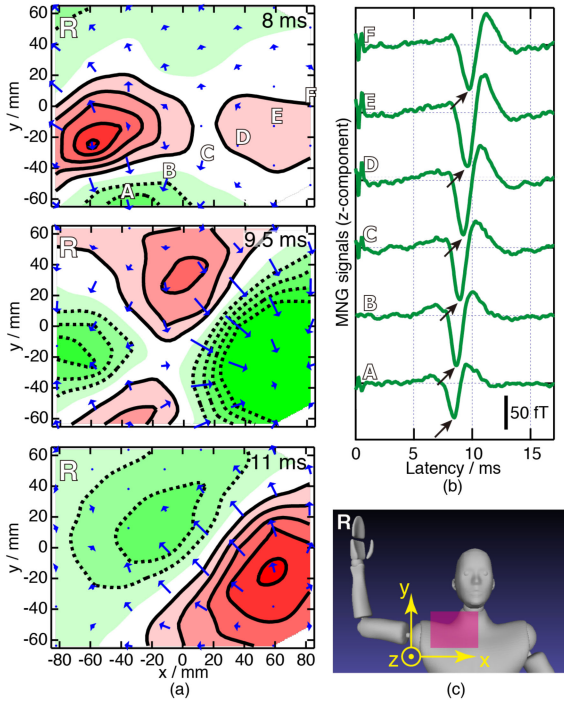


Fig. 5. (a) Example of the transition of the distribution of the magnetic field in the right clavicle area induced by right median nerve stimulation. In the isofield contour maps, plain and dotted lines represent the outward and inward magnetic fields, respectively. The interval between the contour lines is 20 fT. Arrows represent the  $B_x$  and  $B_y$  components. (b) MNG signal waveforms obtained from the sensors labeled in the top contour map in (a). (c) Schema indicating the position of the right clavicle area.

from both the lateral and front sides for further magnetic source analysis.

The median nerves at the wrists were stimulated by repetitive electric current pulses with an intensity of 8–10 mA and a duration of 0.3 ms. The repetition rate was 5 Hz. The magnetic field induced by the stimulation was captured in the vicinity of the ipsilateral clavicle. The signals from the SQUID flux sensors were filtered with a band of 100–5000 Hz and digitized at a sampling rate of 40 kHz. Following the digitization, 2000 epochs were collected and averaged to improve the signal-to-noise ratio.

After averaging, the artifact of the electric stimulation was removed from the obtained signals via dual signal subspace projection (DSSP) [12], and then a magnetic source analysis using a signal space filtering algorithm called the recursive null steering (RENS) spatial filter [13] was used to estimate the current distribution in the observation area.

#### IV. RESULTS AND DISCUSSION

We obtained clear MNG signals from both the right and left arms of both subjects. Fig. 5(a) presents the transition of the magnetic field distribution obtained from the right clavicle area (Fig. 5(c)) of one of the subjects. As shown in Fig. 5(a), the moving quadrupole pattern, which is the typical pattern of the magnetic field from the axonal conduction [20], passing from the left-bottom corner to the right-top corner of the figures was observed. From A to F, the latency of the negative peaks marked by the arrows in Fig. 5(b) shifted later.

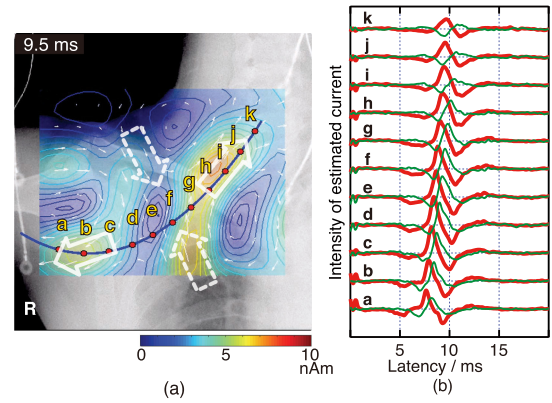


Fig. 6. (a) Estimated current distribution obtained by the RENS spatial filter applied to the magnetic field distribution at 9.5 ms in Fig. 5(a). (b) Waveforms of estimated currents at the positions labeled a–k in (a). The bold red curves indicate the component tangential to the blue curve in (a). The direction from a to k corresponds to positive. The thin green curves indicate the component radial to the blue curve. The positive direction corresponds to the inward direction.

Figure 6 shows an example of the distribution of the current estimated by the RENS filter superimposed on the X-ray image of the clavicle area. The blue curve corresponds to the neural conduction pathway from the median nerve to the spine assumed according to the anatomical structure in the X-ray image obtained from each subject. In addition to the leading and trailing current components along the blue curve, which are indicated by the white hollow arrows, the inward current components at the depolarization site, which are indicated by the dotted hollow arrows, were clearly observed. Fig. 6(b) shows the waveforms of the estimated current at the red dots placed along the blue curve. The peak shifts in Figs. 5(b) and 6(b) indicated signal conduction along the conduction pathway. The conduction velocity estimated from the four arms of the two subjects was  $72.6 \pm 3.6$  m/s on average. This value was physiologically consistent. These results agreed well with a previous study of that recorded the brachial plexus MNG for subjects whose arms were in a neutral position [15].

#### V. CONCLUSION

We developed a new MNG system with improvements in the SQUID sensor array and the cryostat relative to our previous prototype. The improved cryostat provided a large clearance from the observation area to the surface of the cylindrical LHe reservoir. This allowed MNG measurements of the brachial plexus of subjects whose arms were in the abduction and external rotation position, which is a typical symptom provocative position of the shoulder. Thus, the new system can be applied to peripheral nerves with symptom-provoking positioning as well as conventional neutral positioning. This indicates that the new system can extend the range of clinical applications of MNG.

#### ACKNOWLEDGMENT

The authors would like to thank Dr. J. Kawai and M. Kawabata for the manufacturing and evaluation of the newly designed SQUID flux sensors. They would also like to thank Editage for the English language editing service.

## REFERENCES

- [1] R. L. Fagaly, "Superconducting quantum interference device instruments and applications," *Rev. Sci. Instrum.*, vol. 77, 2006, Art. no. 101101.
- [2] E. Boto *et al.*, "A new generation of magnetoencephalography: Room temperature measurements using optically-pumping magnetometers," *Neuroimage*, vol. 149, pp. 404–414, 2017.
- [3] H. Karo and I. Sasada, "Magneto-cardiogram measured by fundamental mode orthogonal fluxgate array," *J. Appl. Phys.*, vol. 117, 2015, Art. no. 17B322.
- [4] Y. Shirai *et al.*, "Magneto-cardiography using a magnetoresistive sensor array," *Int. Heart. J.*, vol. 60, no. 1, pp. 50–54, 2019.
- [5] Y. Adachi, J. Kawai, M. Miyamoto, G. Uehara, H. Ogata, and S. Kawabata, "Multichannel SQUID system for measurement of spinal cord evoked magnetic field for supine subjects," *J. Phys.: Conf. Ser.*, vol. 97, 2008, Art. no. 012281.
- [6] S. Sumiya *et al.*, "Magneto-spinography visualizes electrophysiological activity in the cervical spinal cord," *Sci. Rep.*, vol. 7, Apr. 2017, Art. no. 2192.
- [7] S. Ushio *et al.*, "Visualization of the electrical activity of the cauda equina using a magneto-spinography system in healthy subjects," *Clin. Neurophys.*, vol. 130, pp. 1–11, 2019.
- [8] L. Trahms, S. N. Ern , Z. Trontelj, G. Curio, and P. Aust, "Biomagnetic functional localization of a peripheral nerve in man," *Biophys. J.*, vol. 55, pp. 1145–1153, 1989.
- [9] R. Hari, J. H llstr m, J. Tiihonen, and S. L. Joutsiniemi, "Multi-channel detection of magnetic compound action fields of median and ulnar nerves," *Electroenceph. Clin. Neurophys.*, vol. 72, pp. 277–280, 1989.
- [10] I. Hashimoto, K. Odaka, T. Gatayama, and S. Yokoyama, "Multichannel measurements of magnetic compound action fields of the median nerve in man," *Electroenceph. Clin. Neurophys.*, vol. 81, pp. 332–336, 1991.
- [11] T. Watanabe, Y. Kawabata, D. Ukegawa, S. Kawabata, Y. Adachi, and K. Sekihara, "Removal of stimulus-induced artifacts in functional spinal cord imaging," in *Proc. 35th Annu. Int. Conf. IEEE Eng. Med. Biol. Soc.*, 2013, pp. 3391–3394.
- [12] K. Sekihara *et al.*, "Dual signal subspace projection (DSSP): A novel algorithm for removing large interference in biomagnetic measurements," *J. Neural. Eng.*, vol. 13, 2016, Art. no. 036007.
- [13] I. Kumihashi and K. Sekihara, "Array-gain constraint minimum-norm spatial filter with recursively updated gram matrix for biomagnetic source imaging," *IEEE Trans. Biomed. Eng.*, vol. 57, no. 6, pp. 1358–1365, Jun. 2010.
- [14] T. Sasaki *et al.*, "Visualization of electrophysiological activity at the carpal tunnel area using magneto-neurography," *Clin. Neurophys.*, vol. 131, pp. 951–957, 2020.
- [15] T. Watanabe *et al.*, "Novel functional imaging technique for the brachial plexus based on magneto-neurography," *Clin. Neurophys.*, vol. 130, pp. 2114–2123, 2019.
- [16] Y. Adachi *et al.*, "Improvement of SQUID magnetometer system for extending application of spinal cord evoked magnetic field measurement," *IEEE Trans. Appl. Supercond.*, vol. 21, no. 3, pp. 485–488, Jun. 2011.
- [17] Y. Adachi *et al.*, "Recent advancement in the SQUID magneto-spinogram system," *Supercond. Sci. Technol.*, vol. 30, 2017, Art. no. 063001.
- [18] S. N. Ern , L. Narici, V. Pizzella, and G. L. Romani, "The positioning problem in biomagnetic measurements: A solution for arrays of superconducting sensors," *IEEE Trans. Magn.*, vol. 23, pp. 1319–1322, Mar. 1987.
- [19] Y. Adachi, S. Kawabata, J. Fujihira, and G. Uehara, "Multi-channel SQUID magneto-spinogram system with closed-cycle helium recondensing," *IEEE Trans. Appl. Supercond.*, vol. 27, no. 4, Jun. 2017, Art. no. 063001.
- [20] I. Hashimoto, T. Mashiko, T. Mizuta, T. Imada, K. Iwase, and H. Okazaki, "Visualization of a moving quadrupole with magnetic measurements of peripheral nerve action fields," *Electroenceph. Clin. Neurophys.*, vol. 93, pp. 459–467, 1994.